Original scientific article

Improving well-being and survival in the 6-OHDA lesion model of Parkinson´s disease in mice: Literature review and step-by-step protocol

by Adriane Guillaumin, Bianca Vlcek and Åsa Wallén-Mackenzie

Department of Organism Biology, Unit of Comparative Physiology, Uppsala University

Correspondence: Åsa Wallén-Mackenzie, mail: asa.mackenzie@ebc.uu.se, Uppsala University, Department of Organism biology, Unit of Comparative Physiology, Norbyvägen 18 A, 752 36 Uppsala, Sweden

Summary

Parkinson's disease (PD) is the most common neurodegenerative motor disorder and primarily affects movement control but also a range of non-motor functions. With unknown etiology and lack of cure, much research is dedicated to unravel pathological mechanisms and improve clinical prospects for symptom alleviation, prevention and treatment. To achieve these goals, animal models intended to represent symptoms similar to those observed in the complex clinical display of PD play a key role. It is important to bear in mind that, in any studies with laboratory animals, it is crucial to take the 3Rs principle (Refine, Reduce, Replace) into account. The main pathology of PD includes degeneration of dopamine neurons in the substantia nigra *pars compacta* (SNc). The 6-hydroxydopamine (6-OHDA) lesion model, in which dopaminergic neurons are chemically destroyed, is often favored as a laboratory model of PD in both rodents and primates. However, while reproducing several features of clinical PD, mice exposed to 6-OHDA frequently experience systemic dysfunction causing premature death. To avoid suffering and unnecessary deaths of laboratory mice, there is a need for improved experimental protocols in accordance with the 3Rs principle. Based on current literature and our own previous experiments, we decided to test the effect of three parameters: 1) reduced dose of the 6-OHDA toxin; 2) daily post-operative care to avoid hypothermia and energy loss; 3) shortened interval from surgical injection of toxin to time of sacrifice.

By implementing a 6-OHDA lesion protocol using a lower dose of toxin than commonly seen in the literature alongside careful post-operative care and decreased time post-injection, a fully recovered weight post-surgery and high survival rate was obtained. This was achieved despite full expression of the 6-OHDA-induced locomotor phenotype. A step-by-step protocol was formulated. Validation using histological analysis confirmed toxin-induced degeneration of midbrain dopamine neurons with concomitant loss of dopaminergic projections in the lesioned hemisphere. Notably, while SNc dopamine neurons were drastically reduced, those located in the ventral tegmental area (VTA) were less affected in a medial[high survival] to lateral[low survival] manner.

The Refine and Reduce parameters of the 3Rs principle in experimental animal welfare were specifically addressed which allowed us to improve well-being and survival of mice while maintaining characteristic parkinsonian features in the 6-OHDA lesion model. A table summarizing current literature on the 6-OHDA model in rodents and our validated step-by-step experimental protocol are provided.

Introduction

Parkinson's disease (PD) is the second most common progressive neurodegenerative disease with a prevalence of 1 to 2 per 1000 (Khan et al. 2019; Obeso et al. 2017; Tysnes and Storstein 2017). PD patients are usually diagnosed around the age of 65 years, when motor symptoms begin to appear. Patients suffer from a progressive slowness in initiating movement, loss of postural reflexes and, with time, a rigidity of muscles. Some, but not all, PD patients also display resting tremor. A characteristic hallmark commonly observed in the brain of PD patients is the presence of so called Lewy bodies, accumulations of a misfolded protein known as α-synuclein (Barker and Williams-Gray 2016; Braak et al. 2003; Schneider and Obeso 2015; Spillantini et al. 1997). Life expectancy is shorter in PD, and many patients experience much suffering due to a broad range of symptoms beyond voluntary motor control, including bladder control, pain, depression and cognitive dysfunction, such as dementia (Armstrong and Okun 2020; Chaudhuri et al. 2006; Kalia and Lang 2015; Park and Stacy 2009; Pfeiffer 2016).

A main pathology of PD is the progressive degeneration of midbrain dopamine (DA) neurons, primarily those located in the substantia nigra *pars compacta* (SNc) (Kordower et al. 2013). DA neuron pathology is a key aspect of the clinical diagnosis of PD as it can be determined by brain imaging analysis such as PET scan (Rispoli et al. 2018). With time, DA neurons of the ventral tegmental area (VTA), that usually show higher resilience to PD, might also degenerate. Loss of VTA DA neurons is often associated with affective and cognitive dysfunction. As the disease progresses, multiple brain systems are affected which leads to an even further increase in symptoms and level of suffering for the patient (Muñoz et al. 2020; Paredes-Rodriguez et al. 2020). Still today, there is no cure for PD.

SNc DA neurons are of particular interest in both clinical and pre-clinical (experimental) research. These neurons project primarily to the caudate putamen, mostly referred to as the dorsal striatum in rodents, forming the nigrostriatal pathway. This pathway is a critical modulator of motor control via the basal ganglia and associated structures (caudate putamen (striatum), globus pallidus and the subthalamic nucleus (STN)) (Graybiel 2000; Sesack and Grace 2010). SNc DA neurons extert a strong impact on movement via the so called direct and indirect pathways of the basal ganglia, where nigrostriatal DA release facilitates movement initi-

ation in normal conditions. In contrast, in the parkinsonian brain, the degeneration of DA neurons in the SNc leads to a progressive loss of DA release in the striatum which in turn causes difficulty in movement initiation via the basal ganglia (Björklund and Dunnett 2007). When the patient becomes aware of movement difficulties, such as difficulty in initiating walking, as much as 50-90% of SNc DA neurons have already been lost (Kordower et al. 2013). Understanding the pathological process of PD, not least to find a cure, but also to allow earlier detection and to enable preventive strategies, is an important goal in PD research (Obeso et al. 2017). In terms of treatment, much effort has been aimed at replacing the loss of DA, either by pharmacological administration of DA or its agonists, or by DA cell replacement. Clinically, the administration of DA agonists along with inhibitors of monoamine oxidase B activity is often used in early stages of PD to improve motor function (Armstrong and Okun 2020; Connolly and Lang 2014). Another important treatment is the administration of levodopa (L-dopa), a precursor to DA, which is highly efficient in alleviating motor symptoms in PD (LeWitt 2015). However, after prolonged use and with the progressive degeneration of neurons, L-dopa administration has the unfortunate side-effect of inducing dyskinesias (Olanow and Stocchi 2018; Yang et al. 2021). Much research is therefore aimed at reducing these side-effects by, for example, implementing continuous, rather than intermittent, L-dopa administration (Senek and Nyholm 2014). Cell replacement is another strongly emerging research field aiming at replacing the degenerated DA neurons with newly generated ones derived from various types of stem cells (Cyranoski 2018; Grealish et al. 2014; Parmar et al. 2020). Yet another type of PD treatment, which is already clinically implemented with a high success rate, is so called deep brain stimulation (DBS). DBS consists of high-frequency electrical stimulation delivered via implanted electrodes positioned in brain areas in which the firing activity has been altered as a consequence of the brain pathology in PD. The two most common brain targets for DBS electrodes in PD are the STN and the globus pallidus, both of which display aberrant activity in PD (Alexander et al. 1990; Eisinger et al. 2019). While providing successful alleviation of motor symptoms, the mechanisms underlying DBS have remained largely unknown (Chiken and Nambu 2016; Herrington et al. 2016; Miocinovic et al. 2013). Further, DBS treatment has in some cases been the cause of adverse behavioral and cognitive side-effects, the reasons of which remain to be

discovered (Accolla and Pollo 2019; Benabid et al. 1994; Heywood and Gill 1997; Kim et al. 2015; Petry-Schmelzer et al. 2019).

Taken together, it is evident that much more knowledge is needed to fully understand the pathological changes underlying PD, both to find new opportunities for prevention and treatment, and to optimize current invervention strategies. Due to the complexity of PD, which affects multiple brain circuits with broad impact on the affected individual´s well-being, whole-animal experimental approaches are crucial. Animal models of PD are commonly based either on gene mutations that have been observed in cohorts of PD patients (e.g. LRRK2, α-synuclein (Dawson et al. 2010)), pharmacological intervention (e.g. reserpine, haloperidol (Lorenc-Koci et al. 1996)), or neurotoxins (e.g. N-methyl-4-phenyl-1,2,3,6-tetrahydropyridine, MPTP; 6-hydroxydopamine, 6-OHDA (Hernandez-Baltazar et al. 2017; Kin et al. 2019)).

Among these experimental PD models, the 6-OHDA lesion model is commonly used when aiming to induce DA neuron degeneration (Boix et al. 2015; Cenci and Björklund 2020; Park et al. 2018; Thiele et al. 2012). The 6-OHDA molecule resembles DA and is taken up by the endogenous cytoplasmic membrane transport machinery present in all catecholaminergic neurons. Inside the cell, two mechanisms of action of 6-OHDA are believed to cause cell death: disturbance of the mitochondrial respiratory chain and auto-oxidation of the 6-OHDA molecule which leads to the production of reactive oxygen species (Blum et al. 2001; Glinka et al. 1997; Hernandez-Baltazar et al. 2017). In the experimental setting, 6-OHDA solution is usually injected unilaterally to allow one side of the brain to remain undisturbed by the deleterious effects of the toxin. Each animal thereby has one hemisphere with an intact midbrain DA system, serving as an internal control, and one hemisphere with a 6-OHDA-lesioned DA system. Upon unilateral injection of 6-OHDA, into either the SNc or the nigrostriatal pathway in the median forebrain bundle (MFB), the rodent displays rotational behavior due to loss of movement control by the lesioned hemisphere. The effect of 6-OHDA-induced lesion is fast, which is beneficial for an acute animal model, but with the drawback of a lack of slowly progressive cell loss which is a core feature of clinical PD. The efficiency of the 6-OHDA-induced lesion can be ascertained in each animal by assessing rotational movement, and its exacerbation by a DA-releasing agent, such as the psychostimulant amphetamine, while the extent of DA neuron degeneration requires

post-mortem brain analysis, usually by the use of histological markers for DA neurons.

The 6-OHDA lesion model is today a classical and frequently implemented model to generate subtypes of symptoms representative of PD in experimental animals, including both rodents and primates. Mice are particularly useful for a range of viral-genetics based experiments due to the abundance of transgenic lines available today which allow chemogenetic and optogenetic control over neuronal activity. The possibility to combine these powerful methods with disease models provides great potential for improving knowledge of how to predict, prevent and treat difficult disorders. This is indeed the case for PD for which animal-based experiments have been essential for the knowledge available today. However, mimicking human disorders in mice is difficult, and toxicity-based models, while replicating several human symptoms, risk harming the animal to an extent that outweighs any gain the model can possibly bring in terms of new knowledge. When it comes to implementing the 6-OHDA lesion model in experimental mice, ethical concerns are therefore raised due to the frequent appearance of post-surgical weight-loss and premature death. Lesioned mice experience difficulty in both feeding and maintaining body temperature (Boix et al. 2015; Masini et al. 2021). Ethical considerations commonly grade the 6-OHDA lesioning in mice as a severe procedure. In accordance with the 3Rs principle (Refine, Reduce, Replace) in experimental animal welfare (European Union 2010; Percie du Sert et al. 2020; Tannenbaum and Bennett 2015), one crucial aspect of using laboratory animals is to strive for protocols that fulfil the Refine and Reduce criteria, minimizing suffering and using sufficient animals to draw relevant and useful conclusions but without sacrificing unneccessary animals.

With our interest in generating an improved protocol for the 6-OHDA lesion model in laboratory mice, we searched the literature for standard doses used in rodents, common time post-lesioning until sacrifice, and procedures of post-operative care. Based on the findings, to create conditions with high survival rate and well-being for 6-OHDA lesioned mice while maintaining efficient degeneration of the midbrain DA system, three refinements were made to the protocol: 1) reduced dose of the toxin; 2) careful post-operative care; 3) reduced post-lesioning time. Analysis of several cohorts of mice demonstrates that these precautions lead to the expected toxin-induced loss of midbrain DA neurons, but instead of premature death, mice recover well, re-gain weight and show high survival rate.

Finally, using a range of DA cell markers, it could be concluded that loss of DA neurons had taken place after two weeks, which makes it possible to shorten the post-operative time substantially. This study contributes to an experimental protocol in which animal safety has been taken into consideration, by outlining detailed improvements in the commonly used 6-OHDA lesion model in laboratory mice.

Material and methods

Animals and groups

Adult C57BL/6NTac (Taconic) male mice (> 8 weeks old) were used to generate and validate a 6-OHDA parkinsonian model. Mice were bred in-house and housed at the animal facility of Uppsala University in GM500 cages (Tecniplast, Italy). Each cage contained bedding (Tapvei, Estonia), nesting (shredded paper) and enrichment (carton house) materials (Brogaarden, Denmark). Mice had access to food pellets (Lantmännen, Sweden) and tap water *ad libitum* in standard humidity (45% relative humidity) and temperature (22°C ±2°C) conditions. The housing room was set on a 12-hour dark/light cycle (light on 6:00 to 18:00) with 30 minutes dawn/nightfall transitions. All animal experimental procedures followed Swedish (Animal Welfare Act SFS 1998:56) and European Union Legislation (European Union 2010).

Three groups of mice are reported (Group#0, Group#1, Group#2). A pilot experiment (referred to as Group#0) is included in this report in which mice received a commonly reported dose of 6-OHDA (2.8 and 3.0 mg/mL free base 6-OHDA; N=6). However, due to premature death, this experimental setup was terminated. The full experimental group (Group#1) instead received 1.85 mg/ml free-base 6-OHDA. Group#1 was divided in one cohort of mice sacrificed two weeks (14 days) after lesioning and a second cohort sacrificed three weeks (21 days) after lesioning. Within each cohort, mice were divided into a 6-OHDA subcohort and a control (vehicle) subcohort. Littermate mice were randomly assigned to the different cohorts and sub-cohorts with a maximum of 5 mice per cage. To complement this experimental group (Group#1), a second batch of mice (Group#2) received 1.85 mg/ml free-base 6-OHDA and was sacrificed two weeks (14 days) after lesioning.

Group#1: N=18. N=11 6-OHDA injected mice: 9 mice for *in situ* hybridization analysis (N=8 after the death of one mouse) and 2 mice for immunohistochemistry analysis; N=7 control mice for *in situ* hybridization analysis. Cohorts and subcohorts for *in situ* hybridization analysis: Two weeks post-lesion, N=4 6-OHDA mice, N=4 control mice. Three weeks post-lesion: N=4 6-OHDA mice, N=3 control mice.

Group#2: N=11 6-OHDA injected mice, sacrificed two weeks post-lesion (N=9 after the death of two mice).

N total (Group#1 + Group#2) = 29 of which N= 22 6-OHDA and 7 controls (vehicle).

Pre-operative care

Two days prior to 6-OHDA injection, sunflower seeds were provided in the home cage to increase body weight and habituate the mice to this food supplement.

6-OHDA lesioning

Mice were anesthetized with a mix of air and isoflurane (4 L/min isoflurane-air mix v/v) and maintained anesthetized with 0.5-2 L/min of isoflurane. Mice were then placed in a stereotaxic apparatus and injected subcutaneously with an anti-inflammatory drug (Carprofen, 5mg/mL; Norocarp). After subcutaneous injection of a topical analgesic (Marcain, 1.5 mg/kg; AstraZeneca), the skin was incised to expose the skull. A hole was drilled above the MFB. Coordinates on the right hemisphere: antero-posterior: -1.20 mm from bregma and medio-lateral: -1.10 mm from the sagittal vein. The 6-OHDA solution was freshly prepared on the day of injection by dissolving 2.2 mg of 6-OHDA-hydrochloride in 0.9% NaCl / 0.02% ascorbic acid solution (vehicle) and protected from the light. For control mice, 1 µL of the vehicle was injected. 1 µL of 6-OHDA solution (1.85 mg/mL) or vehicle was injected with a NanoFil syringe (World Precision Instruments, Sarasota, FL, USA) at 100 nl/min, at -4.75 mm from the brain's surface. After 10 min, the needle was slowly removed and the skin stitched. Mice received another injection of Carprofen 20-24 hours after the surgery. A step-by-step protocol is provided in Additional File 1.

Post-operative care

Following surgery, the weight of the mice was monitored daily. Mice administered with 6-OHDA received subcutaneous injections of pre-heated saline (35-37°C, 1 mL) every day until sacrifice to prevent dehydration and hypothermia. In addition, to provide easily accessible food in the home-cage environment, food pellets immersed in a 15% sucrose solution were placed on the floor of the home cage as well as a petri dish filled with the same sucrose solution. Sunflower seeds were placed in the cage a couple of days prior surgery and after surgery until sacrifice.

Nutritionally fortified water gel was also placed in the home-cage for easy access to prevent dehydration and allow weight preservation and/or gain.

Tissue preparation

Two or three weeks after 6-OHDA injections mice were sacrificed by cervical dislocation. Brains intended for histological analysis by *in situ* hybiridzation were frozen in -30 to -35°C 2-methylbutane (≥99%, Honeywell) and stored at -80°C until sectioned with a cryostat (Leica Microsystems, Germany). For histological analysis by immunohistochemistry, whole-animal perfusion with 1X phosphate buffer saline (PBS) followed by ice-cold 4% formaldehyde (FA) was performed, whereupon brains were extracted, post-fixed in 4% FA for 24 hours and cut with a vibratome (Leica Microsystems, Germany).

Immunohistochemistry

60 μm-thick coronal brain sections were washed and incubated for 15 min in a 1% hydrogen peroxidase solution diluted in 1X PBS 0.3% TritonX-100 (0.3% PBST) at room temperature (RT). After rinsing, sections were incubated for 90 min in a blocking solution containing 5 % normal donkey serum (NDS, Millipore) and 0.3% PBST. Sections were then incubated with a primary antibody, rabbit anti-tyrosine hydroxylase (anti-TH, 1:4000, AB152, Millipore), diluted in 0.3% PBST and 1% NDS overnight at 4°C. The next day, sections were rinsed in 1X PBS and then incubated with a secondary antibody, donkey anti-rabbit biotin-SP-conjugated (1:1000, AP182B, Millipore), diluted in 0.3% PBST for 90 min at RT. After washes, an avidin/biotin-based peroxidase system (Vector ABC kit PK-6100, Vector Laboratories) was used to amplify the signal for 90 min followed by a pre-wash in Tris 0.1 M pH7.4 for 10 min. Sections were incubated in a DAB peroxidase solution (SK-4100, Vector Laboratories). Sections were then washed in Tris 0.1 M pH7.4 for 10 min followed by two more washes in 1X PBS. The sections were mounted on glass slides, counterstained with cresyl violet, dehydrated with increasing concentrations of ethanol and mounted with a mounting medium (Leica CV Mount). Sections were scanned with NanoZoomer 2-0-HT.0 and visualized with NDP.view2 software (Hamamatsu).

Fluorescent *in situ* hybridization

16 μm-thin coronal sections were cut using the cryostat and mounted on glass slides for fluorescent *in situ* hybridization, FISH. To allow detection of two mRNAs in the same section, the protocol outlined below (and fully available in (Viereckel et al. 2016)) was implemented. FISH experiments were performed to detect the following mRNAs: Aldehyde dehydrogenase 1 (Aldh1a1), Calbindin1 (Calb1), Gastrin-releasing peptide (Grp) and Vesicular monoamine transporter 2 (Vmat2), all co-analyzed with Th mRNA. Probe design was made by Oramacell and described previously (Dumas and Wallén-Mackenzie 2019). The mRNA sequences detected by the riboprobes were: Th: NM_012740.3; bases 456-1453. Vmat2: NM_013031.1; bases 700-1440. Calb1: NM_009788.4; bases 79-870. Grp: NM_175012.4; bases 127-851. Aldh1a1: NM_001361503.1; bases 1895-2893.

Sections were thawed and post-fixed in 4% paraformaldehyde (4% PFA) for 10 min at RT. After washes in 1X PBS, sections were incubated in a triethanolamine solution (TEA, pH 8) for 5 min followed by incubation in acetic anhydrade-containing TEA solution. Riboprobes (Digoxigenin (DIG)-labelled riboprobe, 50-75 ng/100 μl and fluorescein-labelled riboprobe, 75-100 ng/100 μl) were denatured in hybridization buffer at 85°C for 10 min and applied on the sections for 16-18 hours incubation at 65°C in a humidified chamber. After hybridization, sections were washed in 65°C saline sodium citrate buffer (SSC) baths (5X SSC followed by 0.2X SSC solutions) and a last wash with a 0.2X SSC at RT. Sections were then washed in 1X maleic acid buffer containing Tween20 (MABT) to decrease the binding of non-specific probes. Fluorescein riboprobe was revealed by incubating the sections in a blocking solution containing a blocking reagent (BR, Roche), heat-inactivated FBS and 5X MAB. Sections were then incubated with an anti-fluorescein horseradish peroxidase conjugated (POD) antibody (Roche) for 1 hour. An amplification step was performed by incubating the slices in TSA-biotin amplification buffer (Perkin Elmer) for 15 min. Fluorescein-TSA-biotin complex was revealed by adding Neutravidin-Oregon Green (Invitrogen) for 15 min. After rinsing the sections in Tween20 PBS (PBST), hydrogen peroxidases were inhibited by incubation in 0.1M glycine (pH 2.1) and 3% hydrogen peroxide (H_2O_2). A similar procedure was followed to subsequently reveal the DIG riboprobe with an anti-DIG-POD antibody diluted in BR solution and TSA buffer plus Cy3 (Perkin Elmer). Sections were incubated for 10 min in 1/50000 DAPI solution and mounted with Fluoromount (Southern Biotech). Slices were scanned with NanoZoomer 2-0-HT.0 scanner using the NDP.scan 3.3 software (Hamamatsu).

Table 1: Summary of current literature on 6-OHDA protocols implemented in experimental mice and rats. NS: not specified; MFB: median forebrain bundle; SNc: substantia nigra pars compacta; VTA: ventral tegmental area; E1: experiment 1; E2: experiment 2; E3: experiment 3; C1: concentration 1; C2: concentration 2; C3: concentration 3; C4: concentration 4; s.c.: subcutaneous; i.p.: intraperitoneal.

Mouse strain	Sex	Concentration of free-base 6-OHDA dose (as stated in paper)	Volume injected	Injection site	Survival rate	Pre- and post-operative care	Reference
Current study:							
C57BL/6NTac	Group#0 (N=6) Male	2.8 and 3.0 mg/ml	1 µl	MFB	50%	Pre-operative care: • Supplementary food (sunflower seeds) 2 days prior to surgery Post-operative care: • Daily monitoring of body weight • S.c. administration of pre-heated saline (35-37°C, 1 mL) every day until sacrifice. Saline was not-pre-heated for Group#0. • Daily provision of 15% sucrose solution and food pellets dipped in 15% sucrose solution, sunflower seeds and nutritionally fortified water gel in home cage	Guillaumin, Vlcek, Wallén-Mackenzie (current study)
	Group#1 (N=11) Male	1.85 mg/ml	1 µl	MFB	90.9%		
	Group#1 + Group#2 (N=22) Male	1.85 mg/ml	1 µl	MFB	86.4%		
Literature review:							
C57BL/6J and Vgat-IRES-Cre (Slc32a1)	Male and female	4.44 mg/ml	1 µl	MFB	NS	Pre-operative care: NS Post-operative care: • Daily monitoring of body weight	Bichler et al. 2021
C57BL/6	Male and female	4 µg/µl	1 µl	Striatum (bilaterally)	95%	Pre-operative care: • Habituation and handling prior to surgery to reduce post-operative stress • Supplementary food starting from 1 week before surgery. Post-operative care: • Daily provision of soft chow pellets combined with diet gel boost (3.69 Kcal/g) or high fat diet (5.24 Kcal/g) or sweetened condensed milk diluted in water (1:1, 1.4 Kcal/g), (5 g/mouse), discontinued upon recovery • S.c. administration of 5% sterile glucose solution (10ml/kg) immediately after surgery • S.c. administration of buprenorphine every 12h for 48h or 72h post-surgery • Housing in warm cabinet (24° C), twice/day health check on the first week and once/day in the second week • Dehydration treatment with fluid therapy such as Ringer's solution, sterile saline or glucose solution s.c. or i.p. • Penis prolapse treatment with lubrication • Urinary tract obstruction treatment with lubrication and local analgesic cream	Masini et al. 2021a l6-

Mouse strain	Sex	Concentration of free-base 6-OHDA dose	Volume injected	Injection site	Survival rate	Pre- and post-operative care	Reference
C57BL/6J	Male and female	15 µg/µl	0.2 µl	MFB	96%	Pre-operative care: • Handling 2 to 3 weeks prior to surgery • High calorie dietary supplement • Additional enrichment (cotton pads, plastic house) Post-operative care: • Heating pad in case of hypothermia • S.c injection of warm saline (twice per day) • Carprofen in case of signs of pain • High calorie dietary supplement • Daily monitoring of body weight and behavior • Hand feeding if necessary, forced feeding if necessary • Genitals checked daily (males)	Koski et al. 2019
C57BL/6	Male	15 mg/ml	0.2 µl	MFB	80%	Pre-operative care: NS Post-operative care: • Recovery gels and sugared milk • One half of the cage kept on heating pads for the entire study • Daily monitoring for 3 weeks following surgery and 300 µl glucose (5%) and 300 µl saline (0.9%) administration s.c. if signs of dehydration and malnutrition present	Rentsch et al. 2019
C57BL/6	NS	0.5 µg/µl (C1) 1 µg/µl (C2) 2 µg/µl (C3) 4 µg/µl (C4)	1 µl	MFB	NS	Pre-operative care: NS Post-operative care: NS	Park et al. 2018
C57BL/6	Male	NS	NS	Striatum	NS	Pre-operative care: NS Post-operative care: NS	Im et al. 2016
C57BL/6J	Male	3.6 mg/ml	1 µl	MFB	NS	Pre-operative care: NS Post-operative care: • Daily monitoring of body weight and assessment for overall health and comfort for 1 week post-surgery • S.c. administration of buprenorphine (0.1 mg/kg) up to twice daily when visible discomfort	Sanders and Jaeger 2016
129P2/OLA Hsd	Female	4 g/l	1 µl	MFB Striatum	NS	Pre-operative care: NS Post-operative care: • S.c. administration of 0.5ml saline/glucose (0.9%) solution immediately after surgery • Paracetamol supplement in drinking water for 48h after surgery • Monitoring post-surgery	Bagga et al. 2015
C57BL/6	Male	3mg/ml	2 x 2 µl	Striatum	NS	Pre-operative care: NS Post-operative care: NS	Stayte et al. 2015

Mouse strain	Sex	Concentration of free-base 6-OHDA dose	Volume injected	Injection site	Survival rate	Pre- and post-operative care	Reference
Rgs5$^{gfp/+}$ C57BL/6	Male	0.3 µg/µl (C1) 0.7 µg/µl (C2) 1 µg/µl (C3) 3.6 µg/µl (C4)	1 µl	MFB	91% (C1, C2 and C3) 80% (C4)	Pre-operative care: NS Post-operative care: • S.c. administration of glucose-saline solution immediately after surgery • Hand feeding of food pellets soaked in 15% sucrose/water solution and high calorie jelly food	Boix et al. 2015
C57BL/6J	Male	4 µg/ul	1 µl	Striatum (bilaterally)	NS	Pre-operative care: NS Post-operative care: NS	Bonito-Oliva et al. 2014
Swiss Albino	Male	20 µg/µl	3 µl	Cerebral ventricle	50%	Pre-operative care: NS Post-operative care: NS	Ribeiro et al. 2013
C57BL/6	Male	6 µl/µg	1 µl 2 x 1.5 µl 1.5 µl	MFB Striatum SNc	83.3% 95% >90%	Pre-operative care: NS Post-operative care: • Daily s.c. administration of glucose solution 4% for 2 weeks • Provision of soluble paracetamol analgesia in the home cage water bottle 1 g/l for 3 days • Health evaluation if weight loss below 85%, euthanasia if appropriate	Heuer et al. 2012
FVB	NS	15 mg/ml	V = 0.2 µl	MFB	NS	Pre-operative care: NS Post-operative care: • Free access to sugared water (10mM), nutra-gel and kitten milk replacement • Daily inspection for 2 weeks • Dehydration treatment with 1ml of Lactated Ringer's solution s.c. for 1 week or until improved symptoms • Penis prolapse treatment with mucol gel and Lactated Ringer's solution • Daily check of body weight	Thiele et al. 2012
C57BL/6	NS	3.2 µg/µl	1 µl 2 x 1 µl 2 x 2 µl 1 µl	MFB Striatum Striatum SNc	E1: 80% E1: >90% E1: 80% E1: >90% E2 and E3: 100%	Pre-operative care: NS Post-operative care: E1: No post-operative care E2 and E3: • S.c. administration of 0.1ml/10g body weight sterile glucose/saline (50mg/ml) immediately after surgery, once a day during the first week and on alternate days for up to 3 weeks when necessary • Provision of food pellets soaked in 15% sugar/water twice a day for 2 weeks • Hand feeding of mice exhibiting difficulties eating • Separation of weaker and stronger mice to avoid competition for food	Francardo et al. 2011
NMRI	Female	1.6 µg/µl	1.5 µl	SNc	NS	Pre-operative care: NS Post-operative care: NS	Grealish et al. 2010
C57BL/6	Male	3.0 µg/µl	1 µl 2 x 2 µl	MFB Striatum	14% 65%	Pre-operative care: NS Post-operative care: NS	Lundblad et al. 2004

Rat strain	Sex	Concentration of free-base 6-OHDA dose	Volume injected	Injection site	Survival rate	Post-operative care	Reference
Athymic nude and Sprague-Dawley rats	Male and female	NS	NS	MFB	NS	<u>Pre-operative care:</u> NS <u>Post-operative care:</u> NS	Grealish et al., 2014
Albino Wistar rats	Male	4 µg/µl 4 µg/µl 6.7 µg/µl	4 µl 4 µl + 4 µl 3 µl	MFB MFB + VTA Striatum	NS NS NS	<u>Pre-operative care:</u> NS <u>Post-operative care:</u> NS	Yuan et al. 2005
Sprague–Dawley rats	Male	7.5 µg/ul	1 µl	MFB	NS	<u>Pre-operative care:</u> NS <u>Post-operative care:</u> NS	Tan et al. 2000

Quantitative analysis of the DA markers was made by manually comparing the mRNA positive cells between the 6-OHDA lesioned side with the intact side. A similar amount of mRNA positive cells on the 6-OHDA lesioned side and the intact side gives a percentage of 100%. A lower percentage indicates decreased gene expression on the lesioned side, in comparison to the intact side. Percentages are indicated by : (-) No neurons or extremely few neurons; (+) More than a few neurons, up to 30% of the intact side; (++) 30-50% compared to intact side; (+++) 50-80% compared to intact side; (++++) More than 80% compared to intact side; (NA) denotes Not applicable: for areas where the mRNA is lacking in the control, in accordance with literature.

Results

Well-being and high survival rate confirmed upon implementation of a low dose 6-OHDA toxin followed by daily post-operative care to prevent dehydration and hypothermia

As reported in the literature, the concentration of 6-OHDA commonly used to create parkinsonian locomotor symptoms in rodents varies from 2.5 to 3.6 mg/ml free-base (Bagga et al. 2015; Francardo et al. 2011; Masini et al. 2021; Sanders and Jaeger 2016). This concentration range tends to cause variable well-being and survival (for literature review, see Table 1). In accordance with published literature, we first tested the doses 2.8 and 3.0 mg/mL in a small group of C57BL/6NTac mice (Referred as Group#0; Table 1). However, the mice did not cope well after the injection of 6-OHDA (Figure 1C, weight curve of Group#0). Only 50% survived, and because they showed weight loss, inactivity and loss of appetite, the mice were sacrificed to avoid suffering (Figure 1C). Instead, we decided to test a lower dose to

improve the protocol, and therefore reduced the concentration to 1.85 mg/ml free-base 6-OHDA.

A cohort of 18 C57BL/6NTac mice (Group#1) was injected with either 6-OHDA or vehicle into the MFB of the right hemisphere and mice were subsequently divided into two groups depending on the duration of protocol, two or three weeks until sacrifice (Figure 1A and Figure 2A). Frequent post-operative side-effects of the 6-OHDA lesioning procedure include dehydration and hypothermia, both of which can be prevented by special care (Boix et al., 2015; Francardo et al., 2011; Table 1). In our experiment, pre-heated saline was therefore injected daily which prevented hypothermia after surgery. Also, for easy access to palatable food and water, sucrose-immersed food pellets and a petri dish filled with sucrose solution were placed on the floor of the home-cage. This enabled the mice to drink and feed without the need for caretaker handling which prevented dehydration and allowed weight gain (Figure 1A-C, Table 1). In accordance with the literature, nutritional supplementation in the form of sunflower seed was provided both pre-and post-surgery, and also gel-embedded nutrients were provided post-surgery (Boix et al., 2015; Felgenhauer et al., 2020; Lecker and Froberg-Fejko, 2016; Rentsch et al., 2019; Thiele et al., 2012; Table 1). Initial weight loss was observed in the first days and a peak of weight loss was reached at day 7 (26%) (Figure 1B-C). However, on subsequent days, body weight rapidly increased resulting in an average weight loss below 15% from day 11 and below 5% at day 15 (Figure 1B-C, Table 1). At 21 days post-surgery, when terminated for analysis, Group#1 mice had recovered their weight. After the analysis of Group#1, a second group (Group#2) was injected with 6-OHDA following the same protocol as for Group#1. The weight curve for Group#2 was similar to Group#1. However, Group#2 showed even less weight loss than Group#1 with a peak of weight loss

at day 6 (15% average weight loss) and a progressive recovery on the subsequent days (Figure 1C, Table 1). The general well-being of the mice surviving treatment with the improved 6-OHDA lesion protocol (Group#1, Group#2) can therefore be considered to have been satisfactory.

All control mice survived (100% survival). Three of the 22 mice injected with 6-OHDA died before the day of sacrifice (one mouse in Group#1 and two in Group#2; Table 1). The survival rate was thereby 86.4% among all 22 6-OHDA-treated mice, and 90.9% among the 11 mice in Group#1 that were processed for histological analysis, see below and Table 1.

A step-by-step protocol for the preparation of mice for surgery and the surgical procedure as well as post-operative care according to the details above is provided for easy download and implementation (Additional File 1).

Validation of the 6-OHDA lesion protocol: Mice displayed spontaneous rotations and the midbrain dopamine system had degenerated in the lesioned hemisphere.

Despite the comparatively low dose of 6-OHDA injected (1.85 mg/ml free-base 6-OHDA), all 22 mice displayed spontaneous ipsilateral rotations, starting directly after the surgery and lasting until sacrifice. The spontaneous rotations functionally confirmed the successful lesion of the nigrostriatal pathway using the injection concentration of 1.85 mg/ml free-base 6-OHDA. Next, to validate the extent of degeneration of DA neurons caused by the induced lesion, brains were analyzed by histological methods.

First, tyrosine hydroxylase (TH), the rate-limiting enzyme in DA synthesis and the most common marker used to visualize midbrain DA neurons and their projections, was analyzed by immunohistochemistry. For each mouse, the 6-OHDA-lesioned side was compared with the non-lesioned side, each animal thus serving as its own control. Compared to the non-lesioned side, the lesioned side of the brain showed a strongly reduced amount of cells positive for TH-immunoreactivity (IR) in the SNc and VTA, demonstrating that DA neurons had degenerated as a consequence of the 6-OHDA-injection (Figure 2B, Supplementary figure 1).

Primarily DA neurons of the SNc were affected by the 6-OHDA injection with very few TH-IR-positive neurons detected on the lesioned side (Figure 2B, Supplementary figure 1). In the VTA, TH-IR was only partially affected (Figure 2A, Supplementary figure 1). The medial nuclei of the VTA, corresponding to the interfascicular nucleus (IF), rostral linear nucleus (RLi) and the medial parts of the paranigral nucleus (PN) and parainterfascicular nucleus (PIF), remained largely intact. In contrast, TH-IR was strongly reduced in the ventral and lateral nuclei of the VTA of the lesioned side. These nuclei correspond to the lateral part of the parabrachial pigmented nucleus (PBP) and ventro-lateral parts of the PN
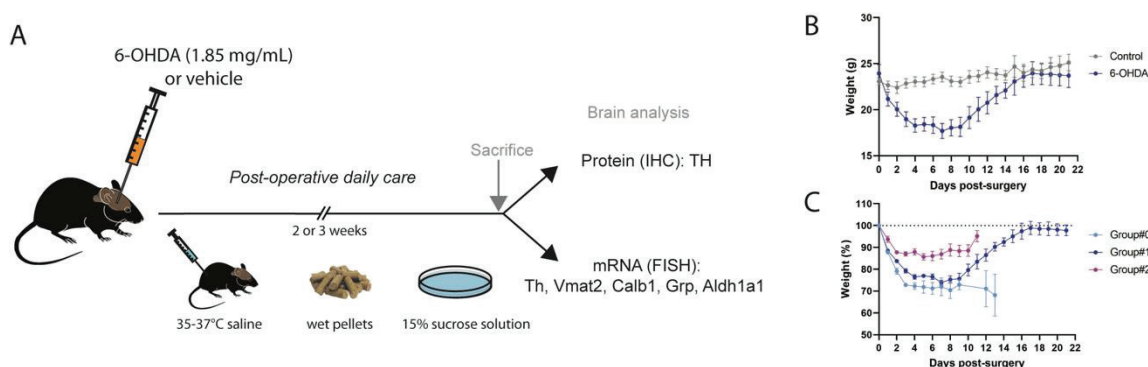
Figure 1: Experimental protocol to induce parkinsonian state in wild-type mice. (A) 6-OHDA or vehicle was injected into the median forebrain bundle (MFB), after which post-operative care included daily subcutaneous injection of warm saline, access to pellets dipped in a 15% sucrose solution, and access to a petri dish filled with 15% sucrose solution placed inside the home cage. Mice were sacrificed two or three weeks after the 6-OHDA injection, and brains extracted. Immunohistochemistry and *in situ* hybridization were performed to detect dopaminergic markers in brain sections covering the midbrain dopamine system. (B) Weight progress of all 6-OHDA lesioned mice and controls mice (N=15 from day 0 to 14; N=8 from day 15 to 21). (C) Percentage of weight for the three experimental 6-OHDA groups: Group#0 high dose toxin (2.8 and 3.0 mg/mL 6-OHDA), and Groups #1 and #2, low dose toxin (1.85 mg/mL 6-OHDA). IHC: immunohistochemistry; FISH: fluorescent *in situ* hybridization.

and PIF (Figure 2B, Supplementary figure 1). Thus, VTA neurons located closest to the SNc were more strongly affected by 6-OHDA than those VTA DA neurons located further away from the SNc and thus closer to the midline. In the VTA, DA neurons thereby showed a medial[high survival] to lateral[low survival] response after 6-OHDA lesioning using the current protocol (Figure 2B).

When addressing TH-positive projections from midbrain DA neurons, a strong decrease throughout the length of the nigrostriatal pathway was observed on the lesioned side. This directly matched the decrease of TH-positive neurons observed in the ventral midbrain (Figure 2B). No TH-positive fibres were visible on the lesioned side in the primary target area of SNc DA neurons, the dorsal aspect of the striatum (dStr) (Figure 2B). VTA neurons project in a topographical manner to the ventral aspect of the striatum (Ikemoto 2007). Medial VTA DA neurons (IF, RLI, medial PN)) project to the medial part of the nucleus accumbens shell (mAcbSh) as well as the

medial part of the olfactory tubercle (OT) while lateral VTA DA neurons (PBP, lateral PN, PIF) project to the ventral part of the nucleus accumbens shell (AcbSh). In accordance with a higher level of DA cell loss in the lateral than medial VTA, TH-positive projections in the ventral part of the AcbSh were substantially fewer on the lesioned side while more preserved in the medial part of the mAcbSh as well as the medial part of the OT (Figure 2B).

TH-positive projections and fibres were preserved in the lesioned hemisphere in structures that are known to be unaffected by the injected 6-OHDA toxin (Supplementary figure 1). This included areas known for receiving dopaminergic input either from other regions than the SNc and VTA, or from noradrenergic (NA) areas (Canteras et al. 1992; Hasue and Shammah-Lagnado 2002; Matthews et al. 2016), including the dorsal part of the bed nucleus of the stria terminalis (BNST), the central nucleus of the amygdala (CeA), and the posterior basolateral nucleus of the amygdala (BLP) (Supplemen-
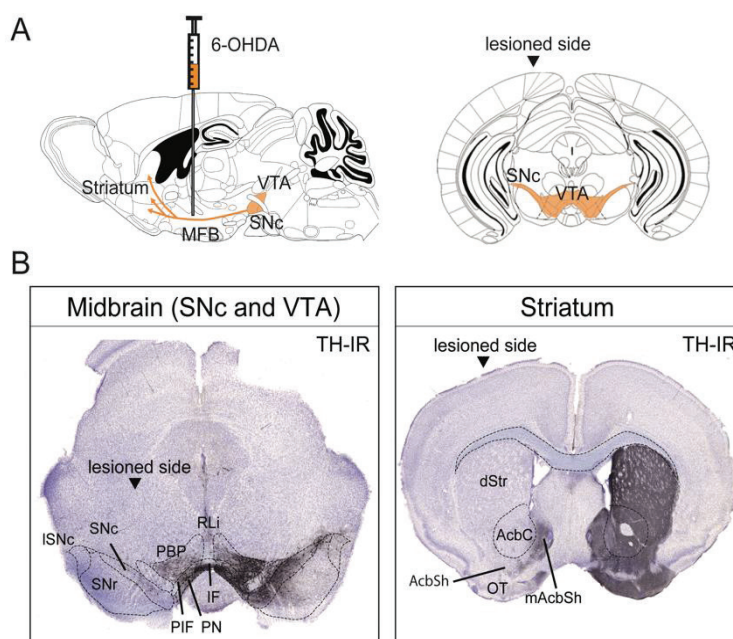
Figure 2: Decrease of TH immunoreactivity in the SNc, VTA, nigrostriatal pathway and striatal complex. (A) Schematique representation of a sagittal section outlining the SNc, VTA, and pathway to the striatum via the median forebrain bundle (MFB) (orange in left picture) with the 6-OHDA (or vehicle) injection in the MFB (left); Coronal representation of SNc and VTA structures, targets of the 6-OHDA injection, outlined in orange (right). (B) Representative immunohistochemistry visualizing dopamine neurons using anti-TH antibody on coronal slices at the midbrain (SNc and VTA) and striatum levels in a 6-OHDA lesioned mouse. VTA subnuclei specified: RLi, IF, PBP, PN, PIF. Striala structures specified: dStr, AcbC, AcbSh, mAcbSh, OT. 6-OHDA lesioned side to the left in the pictures. 6-OHDA: 6-hydroxydopamine; TH: tyrosine hydroxylase; lSNc: lateral substantia nigra *pars compacta*; SNc: substantia nigra pars compacta; SNr: substantia nigra pars reticulata; PBP: parabrachial pigmented nucleus; PIF: parainterfascicular nucleus; PN: paranigral nucleus; IF: interfascicular nucleus; RLi: rostral linear nucleus; dStr: dorsal striatum; AcbC: nucleus accumbens core; mAcbSh: medial part of the nucleus accumbens shell; OT: olfactory tubercle.
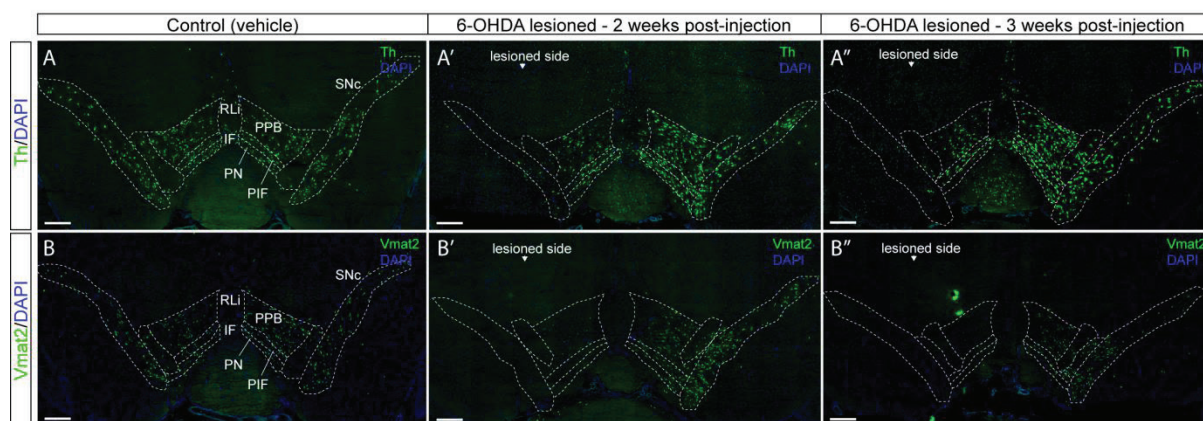
Figure 3: Decrease of Th and Vmat2 mRNAs in both SNc and VTA in the 6-OHDA-lesioned hemisphere. VTA subnuclei specified: RLi, IF, PBP, PN, PIF. 6-OHDA lesioned side to the left in the pictures. DAPI used for nuclear staining. (A and B) Detection of Th mRNA (A) and Vmat2 mRNA (B) in the SNc and VTA in control mice. (A' and B') Detection of Th mRNA (A') and Vmat2 mRNA (B') in the SNc and VTA in 6-OHDA injected mice, 2 weeks post-lesion. (A" and B") Detection of Th mRNA (A") and Vmat2 mRNA (B") in the SNc and VTA in 6-OHDA injected mice, 3 weeks post-lesion. Scale bar: 500 μm. Th: Tyrosine hydroxylase; Vmat2: vesicular monoamine transporter 2; SNc: substantia nigra *pars compacta*; PBP: parabrachial pigmented nucleus; PIF: parainterfascicular nucleus; PN: paranigral nucleus; IF: interfascicular nucleus; RLi: rostral linear nucleus.

tary figure 1). In accordance with the preservation of these TH-positive fibres, TH-positive cell bodies were found in the paraventricular part of the posterior hypothalamus (PH), the periaqueductal grey matter (PAG), the dorsal raphe nucleus (DRN) and the locus coeruleus (LC) (Supplementary figure 1).

The decrease of TH protein upon 6-OHDA lesioning was confirmed by fluorescent *in situ* hybridization (FISH) experiments validating the presence of Th mRNA (Figure 3). In addition to Th, Vmat2 mRNA, encoding the Vesicular monoamine transporter (VMAT2) was assessed.

In the non-lesioned side of 6-OHDA-treated mice (Figure 3, Supplementary figure 2), and in control mice (vehicle-treated; Figure 3, Supplementary figure 2), both Th and Vmat2 mRNA were present throughout the SNc and VTA. This is in accordance with the literature (Adelbrecht et al., 1996; Morales and Margolis, 2017). On the lesioned side, however, a strong reduction of both Th and Vmat2 mRNAs was observed. This was most prominent in the SNc, where no or only few, Th-positive or Vmat2-positive neurons could be observed, thus further validating the success of our modified protocol for the 6-OHDA lesion model. When comparing mice sacrificed two and three weeks post-injection, the same amount of labeling was observed for both Th and Vmat2 mRNAs (Figure 3A'-A", 3B'-B"). In both these cohorts of mice, no or very little labeling for Th or

Vmat2 could be observed in the SNc on the lesioned side while the non-lesioned side remained intact. Thus, there is no difference in detection levels for Th or Vmat2 mRNAs after two weeks post-injection and when mice have been kept alive for three weeks after the injection (Figure 3A-B for controls, 3A'-B' for two weeks post-injection and 3A"-B" for three weeks post-injection).

Calb1, Grp and Aldh1a1 mRNA detection levels were decreased in the SNc and VTA in the lesioned side both two and three weeks after 6-OHDA injection.

Next, we used three different molecular markers for subtypes of SNc and VTA DA neurons: Calbindin 1 (Calb1), Gastrin-releasing peptide (Grp) and Aldehyde dehydrogenase 1 (Aldh1a1). Aldh1a1 has been described as primarily detected in DA neurons of the medial SNc and the immediately adjoining ventral aspect of the VTA; Calb1 is commonly used to define a subtype of DA neurons primarily located in the VTA, but also present in the SNc; Grp has been reported in a spatially restricted subtype of VTA DA neurons and rare SNc neurons (Chung et al. 2005; Greene et al. 2005; Poulin et al. 2018, 2014; Serra et al. 2021; Viereckel et al. 2016).

First, we verified the detection of SNc and VTA DA neuronal subtypes as described in the litera-

ture in control mice and in the non-lesioned side of 6-OHDA injected mice. Here, Calb1 mRNA was confirmed to be present in all VTA subareas and to a much lesser extent in the SNc as previously shown (Poulin et al. 2014; Viereckel et al. 2016) (Figure 4A and Supplementary figure 2). Grp mRNA was found in sparse neurons spatially confined to primarily the medio-ventral aspect of the VTA, and in rare SNc neurons in accordance with the literature (Viereckel et al. 2016). Grp mRNA was strongest in the PN, PIF and IF with weaker density in the PBP (Figure 4B and Supplementary figure 2). Aldh1a1 mRNA was detected in both the SNc and VTA with a higher density in the ventral SNc and ventral aspect of the VTA; a lower density was detected in the dorsal PBP and lateral SNc (Figure 4C and Supplementary figure 2). Thus, in control mice, the patterns observed with these molecular markers were the same as described in the literature (Poulin et al. 2018, 2014; Viereckel et al. 2016).

In contrast, all three molecular markers of VTA and SNc DA neuronal subtypes were strongly decreased in the 6-OHDA lesioned mice, primarily in the SNc (Figure 4A-C; Supplementary figure 2). Quantification of the amount of labeled neurons in the lesioned compared to non-lesioned side is presented in Table 2.

The duration of the protocol (two or three weeks) did not visibly affect the severity of the lesion as detected by these markers. Instead, in both the two-week group and three-week group, the mRNA detection levels of the three markers were similar. Calb1 mRNA was nearly absent in the SNc and strongly decreased in the VTA of the lesioned hem-

isphere, particularly in the lateral parts of the PBP and ventral parts of the PN and PIF (Figure 4A and Supplementary figure 2D-D", 2G-G"). Grp mRNA was somewhat decreased in PBP and ventro-lateral parts of the PN and PIF and lost in SNc (Figure 4B and Supplementary figure 2E-E", 2H-H"). Aldh1a1 mRNA was decreased in both SNc and VTA in the lesioned hemisphere, however, some Aldh1a1-positive cells could be detected (Figure 4C and Supplementary figure 2F-F", 4I-I"). Taken together with the results of Th and Vmat2 above, these findings verify a substantial decrease of all markers analyzed for DA neurons in the SNc, with prominent impact also on VTA DA neurons, in the presented 6-OHDA lesion protocol.

Discussion

In this study, we investigated how well-being and survival of mice treated with the 6-OHDA toxin to generate parkinsonian symptoms could be improved. This is important as data reliability is severely reduced if mice suffer, or even die, during experimental procedures. Even more importantly, from ethical and moral standpoints, experimental protocols that reduce suffering of laboratory animals are needed. In this study, the Refine and Reduce parameters of the 3Rs principle in experimental animal welfare (Tannenbaum and Bennett 2015) were specifically addressed. By improving well-being and survival, the presented protocol will allow researchers to maintain a high quality of life for mice in the 6-OHDA lesion model while also securing reliable data so that fewer mice can be used and unnecessary deaths avoided.

Table 2: Quantitative analysis of SNc and VTA dopamine cell markers in 6-OHDA-treated mice. The table represents the quantified amount of neurons that are left in the lesioned side compared to the non-lesioned, intact, side, as assessed by manual counting. (0) No neurons or very few neurons left; (+) More than a few neurons, up to 30% compared to intact side; (++) 30-50% of the amount on the intact side; (+++) 50-80% of the amount on the intact side; (++++) More than 80% of the amount in the intact side; (NA) Not applicable, applies to areas where the specified mRNA is lacking (in accordance with previous literature). PBP: parabrachial pigmented nucleus; VTAR: ventral tegmental area, rostral part; PN: paranigral nucleus ; PIF: parainterfascicular nucleus; IF: interfascicular nucleus; RLi: rostral linear nucleus ; SNc: substantia nigra *pars compacta*.

mRNA	SNc	VTA			
		PBP + VTAR	PN + PIF	IF	RLi
Th	+	++	+++	+++	+++
Vmat2	0	+	+	++	++
Aldh1a1	+	+	+++	+++	NA
Calb1	0	++	++	+++	+++
Grp	0	+++	+++	+++	NA

We tested changing three critical experimental parameters in order to improve well-being and survival of mice while also improving the experimental protocol and its reproducibility for researchers. Based on current literature, we introduced changes that would affect several phases of the experimental procedure. The changes were: 1) reduced dose of the 6-OHDA toxin; 2) careful post-surgery care (nutrition and warmth); 3) reduced time until sacrifice. The results clearly show that mice coped well when administered a lower dose than commonly used despite displaying the characteristic signs (rotations) of 6-OHDA-induced motor impairment. A high survival rate was observed, while effectiveness of the toxin could be confirmed by histological analysis upon sacrifice, both two and three weeks post-lesion. Using a range of molecular markers, including some of the recently described markers for subtypes
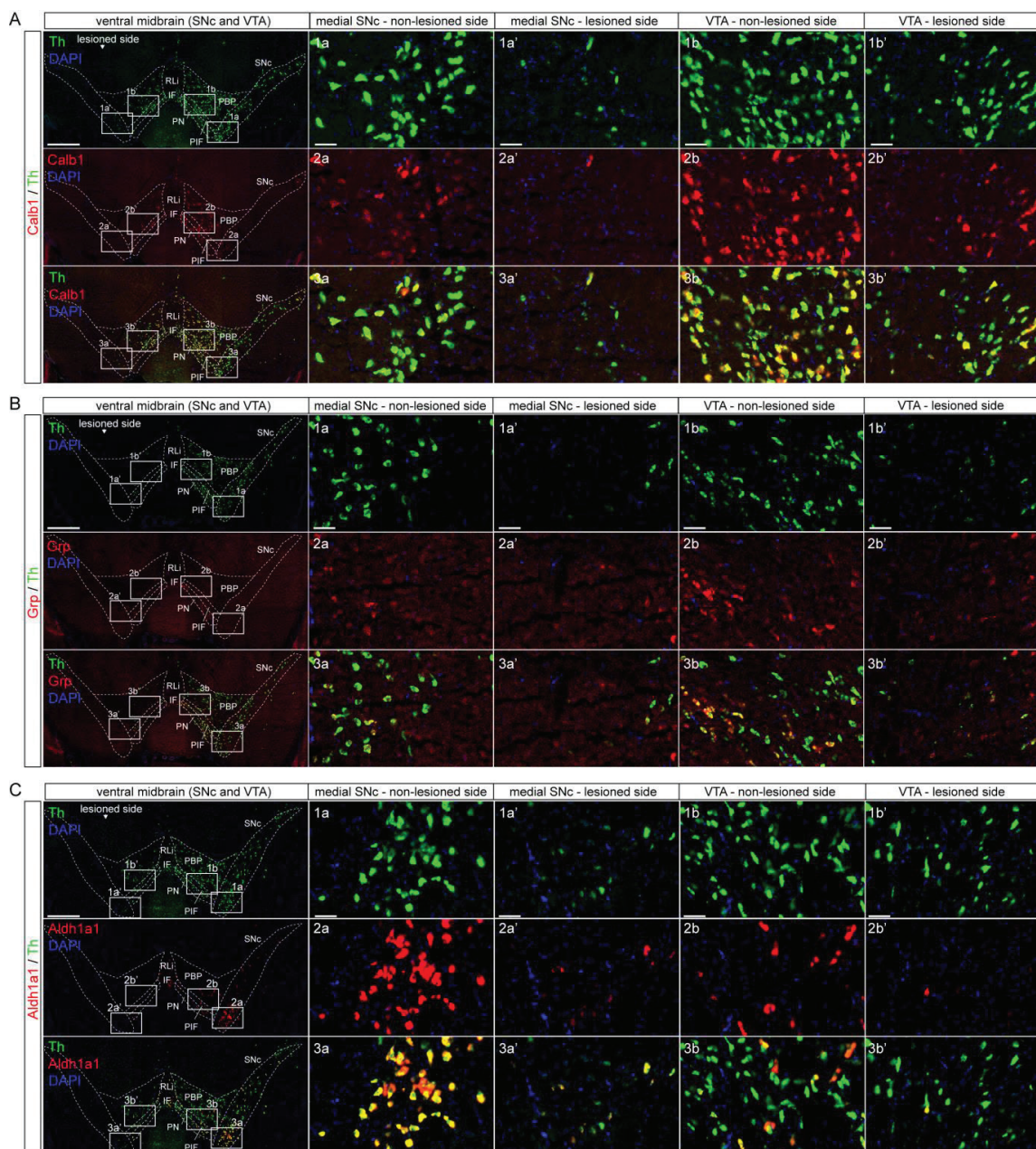
Figure 4: Decrease of DA cell markers Calb1, Aldh1a1, Grp mRNAs in the SNc and VTA in the lesioned hemisphere.
6-OHDA lesioned side to the left in the pictures. Co-localization with Th mRNA (green) for all mRNAs (red) for visualization of dopamine cell bodies. Yellow shows co-localization Th mRNA with the selected mRNA. DAPI (blue) used for nuclear staining. (A) Calb1 mRNA (red) detection in the SNc and VTA in control and 6-OHDA lesioned mice. (B) Grp mRNA (red) detection in the SNc and VTA in control and 6-OHDA lesioned mice. (C) Aldh1a1 mRNA (red) detection in the SNc and VTA in control and 6-OHDA lesioned mice. Th: tyrosine hydroxylase; PBP: parabrachial pigmented nucleus; VTA: ventral tegmental area; PN: paranigral nucleus; PIF: parainterfascicular nucleus; IF: interfascicular nucleus; RLi: rostral linear nucleus ; SNc: substantia nigra pars compacta. All 6-OHDA lesioned data presented here are from the 3 weeks post-injection group. Scale: whole midbrain images: 500μm, close-ups: 50 μm.

of dopamine neurons, the protocol was carefully validated.

In accordance with the Reduce parameter, a limited number of mice were used for the study while maintaining the number necessary to produce results sufficient to draw relevant conclusions. 22 mice were used for the lesion protocol including motor assessment; 10 of these mice were investigated histologically. A step-by-step protocol detailing the precautions taken is provided here to allow any researcher to follow the same procedure. We believe that this protocol should prove beneficial to researchers wanting to study various aspects of PD using mice, not least in the combination with viral-genetics methodology such as optogenetics, chemogenics and various fluorescent probes. The protocol was developed using wild-type C57BL/6NTac mice, but it should be applicable to other mouse strains following testing and validation.

The 6-OHDA parkinsonian model is long-established to induce strong impairments in locomotion. However, due to toxin-induced difficulties in feeding and hydration, current literature clearly shows that animals commonly fail to thrive and that the survival rate can be disturbingly low (Table 1). To improve well-being and survival, addressing the Refine parameter is crucial. By improving post-operative care, as indicated by recent literature (Boix et al. 2015; Francardo et al. 2011; Rentsch et al. 2019), to include prevention of hypothermia by subcutaneous injection of pre-heated saline solution, and by providing nutrition in different forms that could readily be obtained by the lesioned mice while in recovery, most mice increased strongly in weight after surgery and appeared healthy upon inspection. Taken together, these precautions, in combination with the low dose of the toxin, likley contributed to the well-being and high level of survival. The 6-OHDA concentration used in this study was 1.85 mg/ml free-base while the usual concentration reported in the literature varies between 2.5 to 3.6 mg/ml free-base (Bagga et al. 2015; Francardo et al. 2011; Sanders and Jaeger 2016). Comparison between results obtained two and three weeks post-surgery confirmed the full expression of the lesion phenotype after two weeks. Thus, it is unnecessary to leave mice lesioned for three weeks when the phenotype has reached completion already after two weeks. This shortening of experimental time post-lesion should be an advantage if an experiment includes subsequent post-mortem analyses, but also for any experiments that require additional procedures, such as combination with other types of surgery and/or functional recordings or assessments.

Furthermore, the two-week protocol should be sufficient for a complete study of down-stream events following DA cell death in this optimized mouse model of PD.

The 6-OHDA lesion caused a strong decrease of TH-IR in the DA cell bodies of the SNc and partially in the VTA, particularly the lateral VTA subnuclei. These results confirmed previous results showing that 6-OHDA injected in the MFB preferentially destroys DA neurons of the SNc compared to VTA DA neurons (Heuer et al. 2012; Tan et al. 2000). The results were confirmed by fluorescent *in situ* hybridization analyzing the presence of Th, Vmat2, Calb1, Grp and Aldh1a1 mRNA, known markers of DA metabolism (Th, Vmat2) as well as subpopulations/subtypes of distinct DA neurons in the VTA and SNc (Calb1, Grp, Aldh1a1) (Chung et al. 2005; Poulin et al. 2014; Viereckel et al. 2016; Serra et al 2021). Indeed, the presence and distribution of all mRNAs analyzed were decreased uniquely on the lesioned side in the SNc and ventro-lateral VTA, demonstrating that this loss of mRNA labeling was due to neuronal degeneration following the 6-OHDA injection. In accordance with the loss of TH-IR in the ventral midbrain (SNc and VTA), TH-positive fibres were nearly absent from the dorsal and ventral striatum in the lesioned hemisphere, with the exception of the medial mAcbSh. However, the maintenance of TH fibres in this area is in accordance with the preservation of DA neurons in the medial VTA, including the IF and medial PN, which project to the mAcbSh (Ikemoto 2007). The decrease of TH observed with the low concentration of 6-OHDA is in accordance with a previous study showing partial loss of TH-IR in mice injected with a 0.7 mg/ml 6-OHDA solution, analysed five weeks post-lesion (Boix et al. 2015). Another study showed a decrease of TH-IR in the striatum one week post-lesion but used a higher concentration of the 6-OHDA toxin (15 mg/mL) (Rentsch et al. 2019). Here, we combined a lower dose of the 6-OHDA toxin with a short interval between injection and sacrifice to optimize the protocol in respect of both well-being and survival, and hence, reliability of the data.

Although the 6-OHDA model mimics many parkinsonian features, it also has limitations. Firstly, it does not induce the formation of Lewy bodies, an important hallmark of PD. Secondly, the 6-OHDA neurotoxin does not pass the blood brain barrier and has to be injected intracerebrally into the dorsal striatum, the MFB or the SNc to induce degeneration of the nigrostriatal pathway and the associated PD-like symptoms. Thirdly, the 6-OHDA model is

acute and does not cause a slow progression of DA neuron degeneration. These limitations are important to bear in mind when interpreting results from this model. However, while not representing the full repertoire of PD pathology observed in humans, the potent degeneration of SNc and VTA DA neurons in the 6-OHDA model makes it attractive for experimental studies centered around the critical aspect of DA cell degeneration in PD. A mouse-based protocol with improved health status for the experimental animals despite substantial DA cell death is therefore important to achieve.

In general, only a limited number of studies using the 6-OHDA model in mice have reported the survival rate of the animals. This makes it difficult for other researchers to assess the severity and replicability of the procedure on the animals in each study. However, upon scrutinizing current literature, we extracted and summarized the descriptions provided in Methods and Results sections of published reports (Table 1). Several studies that have used the 6-OHDA lesion model in mice or rats were addressed. However, due to lack of information provided in many studies using a 6-OHDA model in rodents, the table may not be complete. Despite the difficulty in comparing studies that have used different conditions (species, injections sites, volume, dose, and various types of post-operative care), we can conclude that the use of post-operative care is essential to reach a high survival rate of mice (80 to 100%). In the present study, we could demonstrate a survival rate of 86.4-90.9% by reducing the concentration of 6-OHDA and implementing post-operative care. Our findings are in accordance with other recent studies that also have aimed to improve survival of mice undergoing the 6-OHDA lesion procedure (Bagga et al. 2015; Boix et al. 2015; Francardo et al. 2011; Grealish et al. 2010; Heuer et al. 2012; Koski et al. 2019; Lundblad et al. 2004; Masini et al. 2021; Rentsch et al. 2019; Sanders and Jaeger 2016; Thiele et al., 2012). The post-operative care employed in our study was mainly based on a literature search performed in 2016, which included the following references: Bagga et al. 2015; Francardo et al. 2011; Grealish et al. 2010; Heuer et al. 2012; Sanders and Jaeger 2016; Thiele et al. 2012. However, more recently , other studies have demonstrated improved protocols that have included additional pre- and post-operative care of the mice (Koski et al. 2019; Masini et al. 2021; Rentsch et al. 2019). These protocols included handling of animals prior to surgery to reduce stress (Koski et al. 2019; Masini et al. 2021) and hand-feeding of animals after surgery to certify their feeding (Boix et al. 2015;

Francardo et al. 2011; Koski et al. 2019). Implementing such precautions might indeed increase survival rate even further, and should be considered for future applications of the 6-OHDA model.

A possible limitation of the present study is the low number of mice used (10 mice for the full procedure including histological analysis; 22 mice in total for assessment of survival rate). However, this limitation is consistent with the animal welfare perspective (3Rs) of reducing the number of animals sacrificed for research purposes, while still obtaining relevant and useful results. Importantly, survival rate indeed increased by using the current protocol. Furthermore, by using a number of different established markers for the DA neuron population, including more recently described markers for subtypes of DA neurons, to maximise the output derived from these experimental mice, the study has allowed detailed histological examination throughout each lesioned mouse brain. Detailed information of the extent of dopaminergic markers in both the SNc and each VTA subnucleus upon implementation of the current 6-OHDA-lesion protocol is thereby available.

In summary, mice coped well throughout the current 6-OHDA lesion protocol, a high survival rate was observed, and the toxin-induced phenotype was confirmed by spontaneous rotations as well as by loss of a range of molecular markers of the midbrain DA system. The current protocol could allow future studies to implement the 6-OHDA mouse model with an improved perpective in terms of animal welfare, and in combination with advanced experimental procedures could help to identify and validate treatment methods for PD.

Conclusions

By here improving the 6-OHDA model in mice, the 3Rs principle (Replace, Refine, Reduce) in experimental animal welfare can be followed more closely, and the Refine and Reduce parameters fulfilled even in advanced experiments aiming to enhance current knowledge and treat complex human disorders.

Ethics approval

The animal study was reviewed and approved by Uppsala Ethical Committee for Laboratory Animal Research (Uppsala djurförsöksetiska nämnd, Uppsala Tingsrätt, Box 1113, 751 41 Uppsala).

Availability of data and materials

Conflict of interests

Funding

Authors' contributions

Acknowledgments

References

Accolla, E.A., Pollo, C., (2019). Mood effects after deep brain stimulation for Parkinson's disease: An update. *Fronties in Neurology*. **10**, 617. https://doi.org/10.3389/fneur.2019.00617

Adelbrecht, C., Agid, Y., Raisman-Vozari, R., (1996). Effect of the weaver mutation on the expression of dopamine membrane transporter, tyrosine hydroxylase and vesicular monoamine transporter in dopaminergic neurons of the substantia nigra and the ventral tegmental area. *Molecular Brain Research*. **43**, 291-300. https://doi.org/10.1016/S0169-328X(96)00214-8

Alexander, G.E., Crutcher, M.D., DeLong, M.R., (1990). Basal ganglia-thalamocortical circuits: parallel substrates for motor, oculomotor, "prefrontal" and "limbic" functions. *Progress in Brain Research*. **85**, 119-146.

Armstrong, M.J., Okun, M.S., (2020). Diagnosis and treatment of Parkinson disease: A review. T*he Journal of the American Medical Association*. **323**, 548. https://doi.org/10.1001/jama.2019.22360

Bagga, V., Dunnett, S.B., Fricker, R.A., (2015). The 6-OHDA mouse model of Parkinson's disease – Terminal striatal lesions provide a superior measure of neuronal loss and replacement than median forebrain bundle lesions. *Behavioural Brain Research*. **288**, 107–117. https://doi.org/10.1016/j.bbr.2015.03.058

Barker, R.A., Williams-Gray, C.H., (2016). Review: The spectrum of clinical features seen with alpha synuclein pathology. *Neuropathology and Applied Neurobiology*. **42**, 6-19. https://doi.org/10.1111/nan.12303

Benabid, A.L., Pollak, P., Gross, C., Hoffmann, D., Benazzouz, A., Gao, D.M., Laurent, A., Gentil, M., Perret, J., (1994). Acute and long-term effects of subthalamic nucleus stimulation in Parkinson's disease. *Stereotactic and Functional Neurosurgery*. **62**, 76–84. https://doi.org/10.1159/000098600

Bichler, E.K., Cavarretta, F., Jaeger, D., (2021). Changes in excitability properties of ventromedial motor thalamic neurons in 6-OHDA lesioned mice. *eNeuro*. **8**. https://doi.org/10.1523/ENEURO.0436-20.2021

Björklund, A., Dunnett, S.B., (2007). Dopamine neuron systems in the brain: an update. *Trends in Neurosciences*. **30**, 194-202. https://doi.org/10.1016/j.tins.2007.03.006

Blum, D., Torch, S., Lambeng, N., Nissou, M.-F., Benabid, A.-L., Sadoul, R., Verna, J.-M., (2001). Molecular pathways involved in the neurotoxicity of 6-OHDA, dopamine and MPTP: contribution to the apoptotic theory in Parkinson's disease. *Progress in Neurobiology*. **65**, 135-172. https://doi.org/10.1016/S0301-0082(01)00003-X

Boix, J., Padel, T., Paul, G., (2015). A partial lesion model of Parkinson's disease in mice – Characterization of a 6-OHDA-induced medial forebrain bundle lesion. *Behavioural Brain Research*. **284**, 196-206. https://doi.org/10.1016/j.bbr.2015.01.053

Bonito-Oliva, A., Masini, D., Fisone, G., (2014). A mouse model of non-motor symptoms in Parkinson's disease: focus on pharmacological interventions targeting affective dysfunctions. *Frontiers in Behavioral Neuroscience*. **8**. https://doi.org/10.3389/fnbeh.2014.00290

Braak, H., Tredici, K.D., Rüb, U., de Vos, R.A.I., Jansen Steur, E.N.H., Braak, E., (2003). Staging of brain pathology related to sporadic Parkinson's disease. *Neurobiology of Aging.* **24**, 197-211. https://doi.org/10.1016/S0197-4580(02)00065-9

Canteras, N.S., Simerly, R.B., Swanson, L.W., (1992). Connections of the posterior nucleus of the amygdala. *Journal of Comparative Neurology.* **324**, 143-179. https://doi.org/10.1002/cne.903240203

Cenci, M.A., Björklund, A., (2020). Animal models for preclinical Parkinson's research: An update and critical appraisal. In: *Progress in Brain Research.* Elsevier, pp. 27-59. https://doi.org/10.1016/bs.pbr.2020.02.003

Chaudhuri, K.R., Healy, D.G., Schapira, A.H., (2006). Non-motor symptoms of Parkinson's disease: diagnosis and management. *The Lancet Neurology.* **5**, 235-245. https://doi.org/10.1016/S1474-4422(06)70373-8

Chiken, S., Nambu, A., (2016). Mechanism of deep brain stimulation: inhibition, excitation, or disruption? *Neuroscientist.* **22**, 313-322. https://doi.org/10.1177/1073858415581986

Chung, C.Y., Seo, H., Sonntag, K.C., Brooks, A., Lin, L., Isacson, O., (2005). Cell type-specific gene expression of midbrain dopaminergic neurons reveals molecules involved in their vulnerability and protection. *Human Molecular Genetics.* **14**, 1709-1725. https://doi.org/10.1093/hmg/ddi178

Connolly, B.S., Lang, A.E., (2014). Pharmacological treatment of Parkinson disease: A review. T*he Journal of the American Medical Association.* **311**, 1670. https://doi.org/10.1001/jama.2014.3654

Cyranoski, D., (2018). 'Reprogrammed' stem cells implanted into patient with Parkinson's disease. *Nature.* d41586-018-07407-9. https://doi.org/10.1038/d41586-018-07407-9

Dawson, T.M., Ko, H.S., Dawson, V.L., (2010). Genetic animal models of Parkinson's disease. *Neuron.* **66**, 646-661. https://doi.org/10.1016/j.neuron.2010.04.034

Dumas, S., Wallén-Mackenzie, Å., (2019). Developmental co-expression of Vglut2 and Nurr1 in a Mes-Di-encephalic continuum preceeds dopamine and glutamate neuron specification. *Frontiers in Cell and Developmental Biology.* **7**, 307. https://doi.org/10.3389/fcell.2019.00307

Eisinger, R.S., Cernera, S., Gittis, A., Gunduz, A., Okun, M.S., (2019). A review of basal ganglia circuits and physiology: Application to deep brain stimulation. *Parkinsonism & Related Disorders.* **59,** 9-20. https://doi.org/10.1016/j.parkreldis.2019.01.009

European Union, (2010). Directive 63/2010 / EU of the European Parliament and of the Council of 22 September 2010 on the protection of animals used for scientific purposes. Official Journal of the European Union L 276 of 20/10/2010.

Felgenhauer, J.L., Brune, J.E., Long, M.E., Manicone, A.M., Chang, M.Y., Brabb, T.L., Altemeier, W.A., Frevert, C.W., (2020). Evaluation of nutritional gel supplementation in C57BL/6J mice infected with mouse-adapted influenza A/PR/8/34 virus. *Comparative Medicine.* **70**, 471–486. https://doi.org/10.30802/AALAS-CM-20-990138

Francardo, V., Recchia, A., Popovic, N., Andersson, D., Nissbrandt, H., Cenci, M.A., (2011). Impact of the lesion procedure on the profiles of motor impairment and molecular responsiveness to L-DOPA in the 6-hydroxydopamine mouse model of Parkinson's disease. *Neurobiology of Disease.* **42**, 327–340. https://doi.org/10.1016/j.nbd.2011.01.024

Glinka, Y., Gassen, M., Youdim, M.B.H., (1997). Mechanism of 6-hydroxydopamine neurotoxicity, in: Riederer, P., Calne, D.B., Horowski, R., Mizuno, Y., Poewe, W., Youdim, M.B.H. (Eds.), Advances in research on neurodegeneration, *Journal of Neural Transmission.* Supplementa. Springer Vienna, Vienna, pp. 55-66. https://doi.org/10.1007/978-3-7091-6842-4_7

Graybiel, A.M., (2000). The basal ganglia. *Current Biology.* **10**, R509–R511. https://doi.org/10.1016/S0960-9822(00)00593-5

Grealish, S., Mattsson, B., Draxler, P., Björklund, A., (2010). Characterisation of behavioural and neurodegenerative changes induced by intranigral 6-hydroxydopamine lesions in a mouse model of Parkinson's disease. *European Journal of Neuroscience.* **31**, 2266-2278. https://doi.org/10.1111/j.1460-9568.2010.07265.x

Grealish, S., Diguet, E., Kirkeby, A., Mattsson, B., Heuer, A., Bramoulle, Y., Van Camp, N., Perrier, A.L., Hantraye, P., Björklund, A., Parmar, M., (2014). Human ESC-derived dopamine neurons show similar preclinical efficacy and potency to fetal neurons when grafted in a rat model of Parkinson's disease. Cell Stem Cell 15, 653–665. https://doi.org/10.1016/j.stem.2014.09.017

Greene, J.G., Dingledine, R., Greenamyre, J.T., (2005). Gene expression profiling of rat midbrain dopamine neurons: implications for selective vulnerability in parkinsonism. *Neurobiology of Disease.* **18**, 19-31. https://doi.org/10.1016/j.nbd.2004.10.003

Hasue, R.H., Shammah-Lagnado, S.J., (2002). Origin of the dopaminergic innervation of the central extended amygdala and accumbens shell: A combined retrograde tracing and immunohistochemical study in the rat. *Journal of Comparative Neurology.* **454**, 15-33. https://doi.org/10.1002/cne.10420

Hernandez-Baltazar, D., Zavala-Flores, L.M., Villanueva-Olivo, A., (2017). The 6-hydroxydopamine model and parkinsonian pathophysiology: Novel findings in an older model. *Neurología* (English Edition). **32**, 533-539. https://doi.org/10.1016/j.nrleng.2015.06.019

Herrington, T.M., Cheng, J.J., Eskandar, E.N., (2016). Mechanisms of deep brain stimulation. *Journal of Neurophysiology.* **115**, 19-38. https://doi.org/10.1152/jn.00281.2015

Heuer, A., Smith, G.A., Lelos, M.J., Lane, E.L., Dunnett, S.B., (2012). Unilateral nigrostriatal 6-hydroxydopamine lesions in mice I: Motor impairments identify extent of dopamine depletion at three different lesion sites. *Behavioural Brain Research*. **228**, 30-43. https://doi.org/10.1016/j.bbr.2011.11.027

Heywood, P., Gill, S., (1997). Bilateral dorsolateral subthalamotomy for advanced Parkinson's disease. *The Lancet*. **350**, 1224. https://doi.org/10.1016/S0140-6736(05)63455-1

Ikemoto, S., (2007). Dopamine reward circuitry: Two projection systems from the ventral midbrain to the nucleus accumbens–olfactory tubercle complex. *Brain Research Reviews*. **56**, 27-78. https://doi.org/10.1016/j.brainresrev.2007.05.004

Im, H.-J., Hahm, J., Kang, H., Choi, H., Lee, H., Hwang, D.W., Kim, E.E., Chung, J.-K., Lee, D.S., (2016). Disrupted brain metabolic connectivity in a 6-OHDA-induced mouse model of Parkinson's disease examined using persistent homology-based analysis. *Scientific Reports*. **6**, 33875. https://doi.org/10.1038/srep33875

Kalia, L.V., Lang, A.E., (2015). Parkinson's disease. *The Lancet*. **386**, 896-912. https://doi.org/10.1016/S0140-6736(14)61393-3

Khan, A.U., Akram, M., Daniyal, M., Zainab, R., (2019). Awareness and current knowledge of Parkinson's disease: a neurodegenerative disorder. *International Journal of Neuroscience*. **129**, 55-93. https://doi.org/10.1080/00207454.2018.1486837

Kim, H.-J., Jeon, B.S., Paek, S.H., (2015). Nonmotor symptoms and subthalamic deep brain stimulation in Parkinson's disease. *The Journal of Molecular Diagnostics*. **8**, 83-91. https://doi.org/10.14802/jmd.15010

Kin, K., Yasuhara, T., Kameda, M., Date, I., (2019). Animal models for Parkinson's disease research: Trends in the 2000s. *International Journal of Molecular Sciences*. **20**, 5402. https://doi.org/10.3390/ijms20215402

Kordower, J.H., Olanow, C.W., Dodiya, H.B., Chu, Y., Beach, T.G., Adler, C.H., Halliday, G.M., Bartus, R.T., (2013). Disease duration and the integrity of the nigrostriatal system in Parkinson's disease. *Brain*. **136**, 2419-2431. https://doi.org/10.1093/brain/awt192

Koski, S.K., Leino, S., Rannanpää, S., Salminen, O., (2019). Implementation of improved postoperative care decreases the mortality rate of operated mice after an abundant 6-hydroxydopamine lesion of nigrostriatal dopaminergic neurons. *Scandinavian Journal of Laboratory Animal Sciences*. **45**, 1-11. https://doi.org/10.23675/SJLAS.V45I0.581

Lecker, J., Froberg-Fejko, K., (2016). Using environmental enrichment and nutritional supplementatioto improve breeding success in rodents. *Laboratory Animals*. **45**, 406-407. https://doi.org/10.1038/laban.1114

LeWitt, P.A., (2015). Levodopa therapy for Parkinson's disease: Pharmacokinetics and pharmacodynamics. *Movement Disorders*. **30**, 64-72. https://doi.org/10.1002/mds.26082

Lorenc-Koci, E., Wolfarth, S., Ossowska, K., (1996). Haloperidol-increased muscle tone in rats as a model of parkinsonian rigidity. *Experimental Brain Research*. **109**. https://doi.org/10.1007/BF00231786

Lundblad, M., Picconi, B., Lindgren, H., Cenci, M.A., (2004). A model of l-DOPA-induced dyskinesia in 6-hydroxydopamine lesioned mice: relation to motor and cellular parameters of nigrostriatal function. *Neurobiology of Disease*. **16**, 110-123. https://doi.org/10.1016/j.nbd.2004.01.007

Masini, D., Plewnia, C., Bertho, M., Scalbert, N., Caggiano, V., Fisone, G., (2021). A Guide to the Generation of a 6-Hydroxydopamine Mouse Model of Parkinson's Disease for the Study of Non-Motor Symptoms. *Biomedicines*. **9**, 598. https://doi.org/10.3390/biomedicines9060598

Matthews, G.A., Nieh, E.H., Vander Weele, C.M., Halbert, S.A., Pradhan, R.V., Yosafat, A.S., Glober, G.F., Izadmehr, E.M., Thomas, R.E., Lacy, G.D., Wildes, C.P., Ungless, M.A., Tye, K.M., (2016). Dorsal raphe dopamine neurons represent the experience of social isolation. *Cell*. **164**, 617-631. https://doi.org/10.1016/j.cell.2015.12.040

Miocinovic, S., Somayajula, S., Chitnis, S., Vitek, J.L., (2013). History, applications, and mechanisms of deep brain stimulation. T*he Journal of the American Medical Association - Neurology*. **70**, 163. https://doi.org/10.1001/2013.jamaneurol.45

Morales, M., Margolis, E.B., (2017). Ventral tegmental area: cellular heterogeneity, connectivity and behaviour. *Nature Reviews Neuroscience*. **18**, 73–85. https://doi.org/10.1038/nrn.2016.165

Muñoz, A., Lopez-Lopez, A., Labandeira, C.M., Labandeira-Garcia, J.L., (2020). Interactions between the serotonergic and other neurotransmitter systems in the basal ganglia: Role in Parkinson's disease and adverse effects of L-DOPA. *Frontiers in Neuroanatomy*. **14**, 26. https://doi.org/10.3389/fnana.2020.00026

Obeso, J.A., Stamelou, M., Goetz, C.G., Poewe, W., Lang, A.E., Weintraub, D., Burn, D., Halliday, G.M., Bezard, E., Przedborski, S., Lehericy, S., Brooks, D.J., Rothwell, J.C., Hallett, M., DeLong, M.R., Marras, C., Tanner, C.M., Ross, G.W., Langston, J.W., Klein, C., Bonifati, V., Jankovic, J., Lozano, A.M., Deuschl, G., Bergman, H., Tolosa, E., Rodriguez-Violante, M., Fahn, S., Postuma, R.B., Berg, D., Marek, K., Standaert, D.G., Surmeier, D.J., Olanow, C.W., Kordower, J.H., Calabresi, P., Schapira, A.H.V., Stoessl, A.J., (2017). Past, present, and future of Parkinson's disease: A special essay on the 200th Anniversary of the Shaking Palsy. *Movement Disorders*. **32**, 1264–1310. https://doi.org/10.1002/mds.27115

Olanow, C.W., Stocchi, F., (2018). Levodopa: A new look at an old friend. *Movement Disorders.*. **33**, 859-866. https://doi.org/10.1002/mds.27216

Paredes-Rodriguez, E., Vegas-Suarez, S., Morera-Herreras, T., De Deurwaerdere, P., Miguelez, C., (2020). The noradrenergic system in Parkinson's disease. *Frontiers in Pharmacology*. **11**, 435. https://doi.org/10.3389/fphar.2020.00435

Park, A., Stacy, M., (2009). Non-motor symptoms in Parkinson's disease. *Journal of Neurology*. **256**, 293-298. https://doi.org/10.1007/s00415-009-5240-1

Park, S.E., Song, K.-I., Kim, H., Chung, S., Youn, I., (2018). Graded 6-OHDA-induced dopamine depletion in the nigrostriatal pathway evokes progressive pathological neuronal activities in the subthalamic nucleus of a hemi-parkinsonian mouse. *Behavioural Brain Research*. **344**, 42–47. https://doi.org/10.1016/j.bbr.2018.02.014

Parmar, M., Grealish, S., Henchcliffe, C., (2020). The future of stem cell therapies for Parkinson disease. *Nature Reviews Neuroscience*. **21**, 103-115. https://doi.org/10.1038/s41583-019-0257-7

Percie du Sert, N., Ahluwalia, A., Alam, S., Avey, M.T., Baker, M., Browne, W.J., Clark, A., Cuthill, I.C., Dirnagl, U., Emerson, M., Garner, P., Holgate, S.T., Howells, D.W., Hurst, V., Karp, N.A., Lazic, S.E., Lidster, K., MacCallum, C.J., Macleod, M., Pearl, E.J., Petersen, O.H., Rawle, F., Reynolds, P., Rooney, K., Sena, E.S., Silberberg, S.D., Steckler, T., Würbel, H., (2020). Reporting animal research: Explanation and elaboration for the ARRIVE guidelines 2.0. *PLoS Biology*. **18**, e3000411. https://doi.org/10.1371/journal.pbio.3000411

Petry-Schmelzer, J.N., Krause, M., Dembek, T.A., Horn, A., Evans, J., Ashkan, K., Rizos, A., Silverdale, M., Schumacher, W., Sack, C., Loehrer, P.A., Fink, G.R., Fonoff, E.T., Martinez-Martin, P., Antonini, A., Barbe, M.T., Visser-Vandewalle, V., Ray-Chaudhuri, K, Timmermann, L., Dafsari, H.S. on behalf of EUROPAR and the IPMDS Non-Motor PD Study Group, (2019). Non-motor outcomes depend on location of neurostimulation in Parkinson's disease. *Brain*. **142**, 3592-3604. https://doi.org/10.1093/brain/awz285

Pfeiffer, R.F., (2016). Non-motor symptoms in Parkinson's disease. *Parkinsonism & Related Disorders*. **22**, S119-S122. https://doi.org/10.1016/j.parkreldis.2015.09.004

Poulin, J.-F., Zou, J., Drouin-Ouellet, J., Kim, K.-Y.A., Cicchetti, F., Awatramani, R.B., (2014). Defining Midbrain Dopaminergic Neuron Diversity by Single-Cell Gene Expression Profiling. *Cell Reports*. **9**, 930-943. https://doi.org/10.1016/j.celrep.2014.10.008

Poulin, J.-F., Caronia, G., Hofer, C., Cui, Q., Helm, B., Ramakrishnan, C., Chan, C.S., Dombeck, D.A., Deisseroth, K., Awatramani, R., (2018). Mapping projections of molecularly defined dopamine neuron subtypes using intersectional genetic approaches. *Nature Neuroscience*. **21**, 1260-1271. https://doi.org/10.1038/s41593-018-0203-4

Rentsch, P., Stayte, S., Morris, G.P., Vissel, B., (2019). Time dependent degeneration of the nigrostriatal tract in mice with 6-OHDA lesioned medial forebrain bundle and the effect of activin A on l-Dopa induced dyskinesia. *BMC Neuroscience*. **20**, 5. https://doi.org/10.1186/s12868-019-0487-7

Ribeiro, R.P., Moreira, E.L.G., Santos, D.B., Colle, D., dos Santos, A.A., Peres, K.C., Figueiredo, C.P., Farina, M., (2013). Probucol affords neuroprotection in a 6-OHDA mouse model of Parkinson's disease. *Neurochemical Research*. **38**, 660-668. https://doi.org/10.1007/s11064-012-0965-0

Rispoli, V., Schreglmann, S.R., Bhatia, K.P., (2018). Neuroimaging advances in Parkinson's disease. *Current Opinion in Neurology*. **31**, 415-424. https://doi.org/10.1097/WCO.0000000000000584

Sanders, T.H., Jaeger, D., (2016). Optogenetic stimulation of cortico-subthalamic projections is sufficient to ameliorate bradykinesia in 6-ohda lesioned mice. *Neurobiology of Disease*. **95**, 225-237. https://doi.org/10.1016/j.nbd.2016.07.021

Schneider, S.A., Obeso, J.A., (2015). Clinical and pathological features of Parkinson's disease In: Nguyen, H.H.P., Cenci, M.A. (Eds.), Behavioral neurobiology of Huntington's disease and Parkinson's disease. Springer Berlin Heidelberg, Berlin, Heidelberg, pp. 205-220. https://doi.org/10.1007/7854_2014_317

Senek, M., Nyholm, D., (2014). Continuous drug delivery in Parkinson's disease. *CNS Drugs*. **28**, 19-27. https://doi.org/10.1007/s40263-013-0127-1

Serra, G.P., Guillaumin, A., Dumas, S., Vlcek, B., Wallén-Mackenzie, Å., (2021). Midbrain dopamine neurons defined by TrpV1 modulate psychomotor behavior. *Frontiers in Neural Circuits*. **15**, 726893. https://doi.org/10.3389/fncir.2021.726893

Sesack, S.R., Grace, A.A., (2010). Cortico-basal ganglia reward network: Microcircuitry. *Neuropsychopharmacology*. **35**, 27-47. https://doi.org/10.1038/npp.2009.93

Spillantini, M.G., Schmidt, M.L., Lee, V.M.-Y., Trojanowski, J.Q., Jakes, R., Goedert, M., (1997). α-Synuclein in Lewy bodies. *Nature*. **388**, 839-840. https://doi.org/10.1038/42166

Stayte, S., Rentsch, P., Li, K.M., Vissel, B., (2015). Activin A protects midbrain neurons in the 6-hydroxydopamine mouse model of Parkinson's disease. *PLoS One*. **10**, e0124325. https://doi.org/10.1371/journal.pone.0124325

Tan, Y., Williams, E.A., Lancia, A.J., Zahm, D.S., (2000). On the altered expression of tyrosine hydroxylase and calbindin-D 28kD immunoreactivities and viability of neurons in the ventral tegmental area of Tsai following injections of 6-hydroxydopamine in the medial forebrain bundle in the rat. *Brain Research*. 869, 56-68. https://doi.org/10.1016/S0006-8993(00)02348-9

Tannenbaum, J., Bennett, B.T., (2015). Russell and Burch's 3Rs then and now: the need for clarity in definition and purpose. *Journal of the American Association for Laboratory Animal Science*. **54**, 120-132.

Thiele, S.L., Warre, R., Nash, J.E., 2012. Development of a Unilaterally-lesioned 6-OHDA Mouse Model of Parkinson's Disease. *Journal of Visualized Experiments*. **3234**. https://doi.org/10.3791/3234

Tysnes, O.-B., Storstein, A., (2017). Epidemiology of Parkinson's disease. *Journal of Neural Transmission*. **124**, 901-905. https://doi.org/10.1007/s00702-017-1686-y

Viereckel, T., Dumas, S., Smith-Anttila, C.J.A., Vlcek, B., Bimpisidis, Z., Lagerström, M.C., Konradsson-Geuken, Å., Wallén-Mackenzie, Å., (2016). Midbrain gene screening identifies a new mesoaccumbal glutamatergic pathway and a marker for dopamine cells neuroprotected in Parkinson's disease. *Scientific Reports*. **6**, 35203. https://doi.org/10.1038/srep35203

Yang, K., Zhao, X., Wang, C., Zeng, C., Luo, Y., Sun, T., (2021). Circuit mechanisms of L-DOPA-Induced dyskinesia (LID). *Frontiers in Neuroscience*. **15**, 614412. https://doi.org/10.3389/fnins.2021.614412

Yuan, H., Sarre, S., Ebinger, G., Michotte, Y., (2005). Histological, behavioural and neurochemical evaluation of medial forebrain bundle and striatal 6-OHDA lesions as rat models of Parkinson's disease. *Journal of Neuroscience Methods*. **144**, 35-45. https://doi.org/10.1016/j.jneumeth.2004.10.004